International Journal of Medicine and Pharmaceutical Sciences (IJMPS)
ISSN(P): 2250-0049; ISSN(E): 2321-0095
Vol. 4, Issue 3, Jun 2014, 91-106

EFFECTS OF STATHMIN N-TERMINAL DOMAIN MUTATIONS ON CELL CYCLE, MICROTUBULES ASSEMBLY AND DYNAMICS IN HELA CELLS

SANA ZOULEYKHA TABET-HELAL BOUALI[1], PATRICK A CURMI[1] & HAFIDA MERZOUK[2]

[1]Laboratory of Normal and Pathological Biomolecules Structure and Activity SABNP, Institute of Health and Medical Research U829- University, Evry Val d'Essonne, France

[2]Laboratory of Physiology, Physiopathology and Biochemistry of Nutrition, Department de Biology, Faculty SNVTU, University of Tlemcen, Algeria

ABSTRACT

Microtubules are major constituents of the cytoskeleton and are involved in many cellular processes such as the formation of the mitotic spindle and intracellular trafficking. These tubular structures, composed by tubulin α/β heterodimers assemble and disassemble with a finely regulated dynamics. Stathmin is a cytosolic phosphoprotein that sequesters tubulin in a non polymerizable complex consisting of two tubulin heterodimers per stathmin molecule (T_2S complex). The I19L (IQVKELEKRASGQAFELIL) peptide derived from the stathmin N-terminal domain corresponds to region folded into a "β-hairpin" structure observed in the T_2S crystals.

To increase the efficiency of this interaction, different mutations were introduced at the level of the I19L peptide and tested *in vitro*. The results showed that the peptideI19L-K4R-A10R is the most effective to inhibit microtubules assembly.

In this work, we introduce these mutations to analyzing their efficiencies on microtubules disassembly and their impact on microtubules dynamic and cell cycle in cancer cell cultures like HeLa.

Over expression experiments of wild-type and stathmin mutant containing the double mutation (K9R-A15R similar to the mutations K4R-A10R for the I19L peptide), suggests that this mutant which is less phosphorylated on serine 16 induces microtubules bundles formation, reduces microtubule dynamics and inhibits cell proliferation.

We thus suggest that we can ameliorate the binding and efficiency of the N-terminal stathmin part by including this double mutation. This variation has an impact *in vitro* and in some cellular aspects such as cell proliferation and microtubules dynamics. These findings may lead to a targeted therapy for this type of cancer.

KEYWORDS: Cell Cycle, HeLa, Microtubule, N-Terminal, Stathmin

INTRODUCTION

Despite significant progress in prevention and diagnosis, cancer still represents an important cause of mortality worldwide. Discovering new drugs and new mechanisms that are more active and more selective might be beneficial in cancer therapy. Therapies intended to block tumor cell cycle or to inhibit tumor cell migration and invasion are also likely to be beneficial and constitute an interesting strategy. The dynamic properties of microtubules (MTs) are crucial for proper cell division and migration, and interfering with them forms the basis of action of one particular cancer treatment (Wang et al., 2011).

MTs are non covalent polymers of the protein tubulin that perform essential transport and structural roles within eukaryotic cells (David-Pfeuty et al., 1977).These cytoskeleton structures have been implicated in vesicle transport, cell structure and motility, signaling, and cell division. The 17-kDa phosphoprote in stathmin (also known as "oncoprotein" 18) (Sobel, 1991), is a tubulin-binding protein involved in the control of MT assembly and dynamic (Belmont and Mitchison, 1996). Originally identified as a key factor in cell proliferation, it also plays roles as a relay protein and integrating protein within intracellular signaling networks. Although it was originally proposed that MTs destabilization by stathmin results from direct "catastrophe" promotion, it is actually due at least in part to sequestration of free tubulin, because stathmin interacts with tubulin in a phosphorylation-dependent manner, to form a T_2S complex of one stathmin (S) and two tubulin heterodimers (T) (Curmi et al., 1997; Jourdain et al., 1997). This controversy was resolved by a study demonstrating that stathmin mediates both "catastrophe" promotion and sequestration of tubulin and that detection of these activities depend on buffer conditions (Howell et al., 1999).Consequently, stathmin has direct effects on cellular processes such as migration, division, and growth cone guidance by influencing the association of MTs with the actin cytoskeleton (Liang et al., 2008).

Phosphorylation of stathmin is observed in response to hormones (Beretta *et al*., 1988), cytokines (le et al., 1991), neurotransmitters (Chneiweiss et al., 1992), and growth and differentiation factors (Doye et al., 1990).

Stathmin is phosphorylated by a variety of extracellular signals and drugs. Serine-16 has been shown to be phosphorylated by the Ca2+/calmoduline dependent kinase IV/Gr (CaMKIV/GR) in T cells stimulated with either the calcium ionophoreionomycin or through the T-cell antigen receptor. Moreover, progression through the cell cycle appears to require multisite phosphorylation of stathmin. It has been shown that over expression of a non phosphorylable mutant of stathmin resulted in a large population of cells blocked in G2/M with a high DNA content (Larsson et al., 1995). However, the molecular mechanism by which stathmin destabilizes MTs still remain unclear.Further, stathmin is the generic element of a protein family, including SCG10 (Superior Cervical Ganglia Protein 10), SCLIP (SCG10-Like Protein) and RB3 (Rat Brain-3), that share a highly conserved SLD (Stathmin-Like Domain). All SLDs domains are able to sequester tubulin in T_2S complex but at variety stabilities (Charbaut et al., 2001). The N-terminal domain of RB3-SLD caps α-tubulin at a position and in a way that may prevent the longitudinal addition of the capped tubulin to the "plus" ends of growing MTs (Steinmetz et al., 2000).The recent crystallographic structure of a tubulin-colchicine/RB3-SLD complex at 3.5 Å, revealed three domains within the SLD : an N-terminal cap domain (residues 4-28), a linker domain (29-45), and a long, mostly α-helical domain (46-145) bearing two duplicated tubulin binding sites (Ravelli et al., 2004).

A closer view of the N-terminal cap domain of RB3-SLD in the tubulin-colchicine/RB3-SLD complex shows the presence of a β-hairpin motif that possesses residues in an interaction with some of the α-tubulin residues involved in the interdimer (Dorleans et al., 2009).

Short and long peptides from N-terminal part of human SLDs domain were studied, the results shows that this peptides impede tubulin polymerization at different stabilities, where the peptide I19L derived from N-terminal region of protein stathmin is the most efficient, suggesting that it adopts a specific folding by the interaction with tubulin. In this case, the β-hairpin structure is stabilized by eight hydrogen bonds between backbone atoms of the two strands. The hydrophobic interactions observed between residues Val-8 (β1) and Leu-22 (β2) and between Leu-11 (β1) and Ala-19 (β2) are also likely to participate in the stabilization of this structure. Finally, the presence of the bulge changes the usual

distribution of side chains alternatively on each side of the α-sheet and brings Glu-10 and Lys-13 side chains close in space, thus allowing an ionic interaction between these residues (Clement et al., 2005). However, a somatic mutation in stathmin gene has been introduced in N-terminal domain at I19L peptide region, which results in substitution of lysine (K) for arginine (R) at amino acid position 4 and substitution of alanine (A) for arginine (R) at amino acid position 10 (K4R-A10R) aimed to stabilize the β hairpin motif. The arginines substituted are able to interact with negatively charged residues present on the surface of tubulin, the fact first mutation (K4R) create a newhydrogenbonding intra-peptide with glutamate 6, the second mutation (K10R) strengthens hydrogen bond with a spartate 46 opposite tubulin which stabilizes the folding of tubulin, in other way this mutation is upstream the first phosporylation site of stathmin, and it may alsointeract with thissite by hydrogen bond.

In this study, we examined *in vitro* the effects of this double mutation (K9R-A15R similar to the mutations K4R-A10R for the I19L peptide) on stathmin N-terminal domain on the polymerization of tubulin, MT dynamic and cell cycle.We therefore suggest those mutations increase stathmin/tubulin interaction binding resulting serine 16 phosphorylation state reductions, MTs bundles formation in mitotic cells, MT dynamic reduction and cell proliferation inhibition.

MATERIALS AND METHODS

Plasmid Constructs

Stathmin cDNAs were amplified by PCR. The 5 ’and 3’ primers were chosen in order to introduce a 5’KpnI and a 3’BamHI restriction site to subclone into the eukaryotic expression vector pEGFP-N1 coding enhanced *green fluorescent protein*(GFP).The DNA oligonucleotides (Sigma) coding Wild-type stathmin and stathmin double mutant were designed and synthesized as follows:

5’cgc **agatct**atggcttcttctgatatccag 3’ Bgl II restriction sites is designed in bold

5’cgc **ggtacc**gcgtcagcttcagtctcgtcagc 3’ Kpn I restriction sites is designed in bold

All these sequences were inserted between Bgl II and Kpn I (Fermentas) restriction sites of pEGFP-N1 plasmid. The recombinant vectors were confirmed by the digestion analysis of restriction endonuclease and DNA sequencing by Beckman Coulter Genomics (United Kingdom).

Cell Culture

HeLa cells were grown in Dulbecco's Modified Eagle Medium (DMEM: Gibco) with 5% fetal calf serum and 1% penicillin/streptomycin (Invitrogen Life Technologies), at 37°C in a humidified atmosphere containing 5% CO_2. All cells were dissociated in 0.25% trypsin (Invitrogen Life Technologies) then diluted 1:10 before replating.

Synchronization and Transfection

For synchronization studies, confluent cultures containing approximately (15 X 10^4 cells/cm^2) were arrested in mitosis by thymidine/nocodazole block (Sigma). Thymidine was added at 0.5 mM and the cultures were incubated at 37°C, after 15h the medium containing the thymidine was removed, the cells were incubated 10h without drug, the nocodazole was added at 30 nM during 12 h. The thymidine was dissolved in 0.5 x Phosphate-Buffered Saline (PBS) and the nocodazole was dissolved in DMSO, both products were kept at -20°c.

For transfection, the cells were watched twice in PBS 1x and DMEM, the transfection was performed using lipofectamine^{TM} 2000 (Invitrogen Life Technologies) combined to 1 µg Stathmin-p-EGFPN1 plasmid (called stathmin-GFP) in the 800 µl Opti-MEM® reduced serum medium. After 20 minutes, the cell culture medium was removed and replaced with DMEM medium without serum and the DNA-lipid Opti-MEM® mixture.

Immunofluorescence

HeLa cells were grown in individual box of 1.9cm^2 (5 X 10^{4}cells/box)in 37°Cand 5%CO_2overnight. The following day, there were transfected with 0.5µg of stathmin-GFP and 1 µl lipofectamine^{TM} 2000 in the 800 µl Opti-MEM® medium. After transfection, HeLa cells growing in plastic dishes were washed with PBS and fixed with 4% paraformaldehyde (PFA) in PBS for 25 min at 37°C. Cells were washed thrice with PBS and incubated for 1h in blocking solution (20 mm Tris-HCl, 150 mm NaCl, 0.1% Triton, 2% BSA, 0.1% Azide, pH 7.4).

The MT network, stathmin immuno-localization and stathmin phosphorylated serine 16 were revealed by immunofluorescence with E7 anti-α-tubulin mouse antibody (1:3000), anti-COOH-terminal (antiserum C) of Stathmin rabbit antibody (1:500) and anti-phosphorylated serine 16 (P16) rabbit antibody (1:10 000).

Cells were washed extensively in PBS and incubated for 2 h with secondary antibodies goat anti-mouse (Alexa Fluor 555, 1:2500 dilution) or goat anti-rabbit (Alexa Fluor 594, 1:2500 dilution) (Molecular Probes) in blocking solution and washed again with PBS. DNA was stained by incubation with DAPI (1:6500) (Invitrogen) for 20 seconds. The cells were finally washed with PBS and examined for fluorescence with a Zeiss microscope using a 63x/1.4 or 100x/1.4 numerical aperture objectives.

Immunoblotting

HeLa Cells were lysed in 50 mM Tris-HCl (pH 7.5), 150 mM NaCl, 0.1% (vol/vol) Triton X-100, 1 mM EDTA, and protease inhibitor cocktail (Roche, Indianapolis, IN). Lysates were centrifuged at 14,000 × *g* for 15 min at 4°C, and supernatants were collected. Proteins were separated on 12% SDS–PAGE gels and transferred onto a nitrocellulose membrane (Invitrogen, Carlsbad, CA). The membranes were blocked in 5% (wt/vol) nonfat dried milk/PBS for 30 min at room temperature and incubated for 1 h at room temperature with primary antibodies (anti-COOH-terminal (antiserum C) of Stathmin rabbit antibody; 1:5000 dilution) and anti-GAPDH used as a protein loading control (1:5000; Abcam). Bound antibodies were detected and quantified with an Odyssey imaging system (LI-COR Biosciences, Lincoln, NE) using anti-rabbit IRDye 800 or anti-goat IRDye 680 secondary antibodies (1:5000 dilution; Odyssey; LI-COR Biosciences).

Cell Proliferation Assay by Mtt (3-(4, 5-Dimethylthiazol-2-Yl)-2, 5-Diphenyl Tetrazolium Bromide)

Three groups of HeLa cells were grown in 24-well plates of 1.9 cm^2 dimension (5x10^4 cells/well), synchronized and transfected. At 19, 24, 35 and 48 h following transfection 40 µl of MTT was added to each well to have 1% final concentration.After 2 h incubation and 37°C in the dark, 400 µl stabilized solution was added to each well for 20 minutes to dissolve the formazan crystals. The absorbance was measured using UV visible spectrophotometer *(Analytik Jena* Instruments, Germany*)* at 570 and 690 nm, the final value is subtracted from the twos absorbance values.

The viability of the transfected cells was represented by optical density (OD) of growth population plus standard error of each mean.

Video Microscopy of MT Dynamic

HeLa cells were grown in individual box 9.6cm^2 dimension (2x10^{5}cells/box) in 37°Cand 5%CO_2overnight. The following day, there were synchronized and transiently co-transfected with stathmin-GFP vector and mcherry-EB3 eukaryotic vector coding enhanced *red fluorescent protein*(RFP), and then cultured for 5 h before real-time monitoring of MT dynamic.

Fluorescence video microscopy was implemented on an inverted microscope (Axiovert 220; Carl Zeiss MicroImaging, Jena, Germany). RFP emission was detected with a 63x/1.4 numerical aperture objective. Time-lapse images were captured at 1-s intervals for 2 min using a Zeiss cooled charge-coupled device camera. To measure MT elongation rates, the distances covered by MT ends were measured by analyzing sequential images with the Manual tracking-Image J software. Ambiguous trajectories were discarded.

Statistical Analysis

All experiments were performed at least in triplicate and all quantitative data are presented as means ± SD. $P < 0.05$ was considered statistically significant.

For MTT, all groups were performed with the One-way analysis of variance (ANOVA) followed by the least significant difference (LSD) test, using STATISTICA version 4.1 (Statsoft, Paris, France).

The average speed of MTs 50 “plus” end movement was analyzed using (Kruskal-Wallis, Nonparametric (ANOVA) test followed by the non-parametric post-hoc Dunn test using STATISTICA version 8.0 (Statsoft, Paris, France) after verification of non-normal distribution of values of each population.

RESULTS

Characterization of Antisera Directed Against the Phosphorylated Sites of Stathmin

To further investigate the function and mechanism of action of wild-type (WT) stathmin and double mutant stathmin (K9R-A15R-stathmin) during the cell cycle, we examined their intracellular localization and expression in synchronized HeLa cells by immunofluorescence microscopy using polyclonal antibodies directed against a COOH-terminal peptide of stathmin (antiserum C) (Koppel et al., 1990). We also generated polyclonal antisera directed against the phosphorylated site 16, (anti-16P, see Materials and methods) to study the subcellular localization and the state of the phosphorylation of these corresponding forms of stathmin.

The results show that anti-stathmin antiserum C yielded a punctate staining in the cytoplasm, which was more concentrated around the nucleus with K9R-A15R-stathmin (Figure 1a).

Both proteins are expressed correctly in HeLa cells indicating their stability; however, the K9R-A15R-stathmin is expressed also at perinuclear area which may it confer a new properties towards the MT network in this area. This is further confirmed by Western blotting, where K9R-A15R-stathmin is more expressed than WT-stathmin at 35 and 48 hours in synchronized HeLa cells (Figure 1b).

We next examined the subcellular localization and the phosphorylation state of stathmin phosphorylated on site 16 in synchronized HeLa cells at different times after transfection. The aim is to analyze the effect of the second mutation (K15R)of K9R-A15R-stathmin on this site phosphorylation state, which it’s upstream.

In interphasic cells, a punctuate staining was very weakly detected with anti-16P in the presence of WT-stathmin or K9R-A15R-stathmin, wherever, mitotic cells were strongly labeled in the presence of WT-stathmin and less labeled in the presence of K9R-A15R-stathmin, in particular at 35 h (Figure 2b-c). The staining of mitotic cells increased from prophase to metaphase and strongly decreased at cytokinesis (Figure 2). The very rapid dephosphorylation of stathmin on site 16 occurs at cytokinesis, as soon as the cells have finished their transition through the mitotic phase (Gavet et al., 1998).

In all experiments, DNA visualized by staining with DAPI is normal, it allowed us to visualize proliferation cellular step, is very likely that the dead cells were detached and could be didn't visualized by immunofluorescence microscopy. These observations indicate that all mitotic cells over expressed K9R-A15R-stathmin are less phosphorylated on site 16 which could be related to its mutations, high expression level and low degradation degree. Furthermore, this low state of phosphorylation could be a result for the stability of the interaction between stathmin and tubulin which is enhanced by the double mutation introduced.

Together, these results suggest that, the double mutation introduced in K9R-A15R-stathmin it has gave distinct properties compared to WT-stathmin such as it subcellular localization, expression and site 16 phosphorylation state.

Effects of Stathmin on the MT Network

Stathmin inhibits MTs polymerization by sequestering tubulin on T_2Scomplexformed by one molecule of stathmin and two heterodimers α-β of tubulin(Curmi et al., 1997;Jourdain et al., 1997).

To investigate the role of WT-stathmin and K9R-A15R-stathmin on MTs depolymerization, we over expressed this forms in synchronized HeLa cells and analyze the MT network at different times by immunofluorescence microscopyusing monoclonal antibodies directed against α-tubulin of MTs (Figure 3).

The results indicate that in mitotic cells, WT-stathmin overexpression didn't induced MTs depolymerization compared to untransfected cells. In contrast, K9R-A15R-stathmin overexpression reorganizes MTs into bundles (asterisks) at perinuclear area (in cytokinesis cells) where it is more localized (Figure 3b-c). DNA stained by incubation with DAPI appears normal; it gave us more detail at the successive steps of mitosis.

Together, these results suggest that, K9R-A15R-stathmin which is more expressed and less phosphorylated had a visible effect on MTs network in mitosis. These observations are correlated with studies showed that the effect on the MT network was clearly dependent on the level of stathmin expression (Gavet et al., 1998).

Effects of Stathmin on Cell Proliferation

During cell cycle, stathmin is phosphorylated allowing the formation of the mitotic spindle and cell cycle progression(Rubin and Atweh, 2004).

To detect the effect of stathmin proteins overexpression on the proliferation of cells, synchronized and transfected HeLa cells were seeded into 24 well plates ($5x10^4$cells/well). Cultures were collected at different time points for analysis of cell proliferation level using MTT assay.

The results show that the proliferation level between the three groups of transfected HeLa cells was different (Figure 4). Both stathmin proteins expressedat19 h, 24 h inhibit cell proliferation more ($P< 0.001$) than the control which contains transfected cells with p-EGFPN1 vector. At 35h, data show a significant difference between WT-stathmin and the

control ($P< 0.01$) and between K9R-A15R-stathmin and the control ($P< 0.001$). At this level, K9R-A15R-stathmin inhibits more cell proliferation than WT-stathmin ($P< 0.001$). At 48 h, the difference exists only between the controlandK9R-A15R-stathmin ($P< 0.05$). At this level, WT-stathmin is less expressed (immunoblotting data). These observations reevaluate the inhibition of cell proliferation byK9R-A15R-stathmin at this moment.

Together, these results suggest that overexpression of stathmin proteins disrupts the cell proliferation with a greater effect for K9R-A15R-stathmin.

Impacts of Stathmin on MT Dynamic

Stathmin is an important regulator of MT polymerization and dynamic (Manna et al., 2009). Analysis of dynamic instability at “plus” and “minus” ends was carried out by video-enhanced differential interference contrast microscopy as previously described (Manna et al., 2006).

We wanted to analyze the ability of stathmin proteins to modulate MT dynamic instability in interphasic HeLa cells by measuring MTs “plus” end moving using the fluorescent protein RFP coding by mcherry-EB3 vector with the particularity to bind to the “plus” end of MTs (Figure 5a).

The elongation rate of MTs was observed in live fluorescence video microscopy and was performed using Kruskal-Wallis, non parametric ANOVA test followed by the non-parametric post-hoc Dunn test.

These results prompted us to further investigate the role of stathmin proteins on the elongation rate of dynamical MT plus ends. Video microscopy of EB3 revealed that the elongation rate of MTs”plus” ends was considerably reduced in the presence of WT-stathmin compared to the control (EB3 alone) ($P< 0.05$) and in the presence of K9R-A15R-stathmin compared to the control ($P< 0.05$). K9R-A15R-stathmin further reduces the elongation rate of MTs “plus” end than WT-stathmin ($P< 0.05$) (Figure 5b).

Together, these results suggest that, the double mutation introduced could stable the interaction between stathmin and tubulin resulting reduction of MT dynamic.

DISCUSSIONS

Stathmin (also called oncoprotein 18 “Op18”), a cytosolic phosphoprotein, is a member of a family of MT-destabilizing proteins that regulate the dynamic of MT polymerization and depolymerization (Mistry and Atweh, 2002). It is organized in two domains witch slightly overlap between amino acids 50-70: an NH2 terminal “regulatory” domain containing several phosphorylation sites and a COOH-terminal “interaction” domain that presents a predicted α-helical structure potentially forming coiled-coil interactions with other proteins (Curmi et al., 1999).

Stathmin is variably phosphorylated on four distinct serine residues in intact cells, namely, Ser-16, -25, -38, and -63 (Beretta et al., 1993;Marklund et al., 1993). All four serine residues are phosphorylated to high stoichiometry during mitosis (Larsson et al., 1995). Stathmin is also element of the generic a conserved protein family including the neural proteins SCG10, SCLIP, RB3 and its two splice variants RB3’ and RB3’’ (Anderson and Axel, 1985;Maucuer et al., 1993;Ozon et al., 1997;Schubart et al., 1989;Stein et al., 1988).

Here, we examined the intracellular localization, expression and MT destabilizing activity of WT-stathmin and K9R-A15R-stathmin *in vivo*, and theirs activity regulation by phosphorylation on site 16 during cell cycle.

We controlled the localization subcellular and the expression of WT-stathmin and K9R-A15R-stathmin in synchronized HeLa cells, the two forms have cytoplasmic localization with could be resulting of the presence of manycharged residuesin its sequence. Stathmin was detected on cytoplasmic fraction, immunofluorescence microscopy in HeLa cells overexpressing stathmin shows a cytoplasmic localization (Gavet et al., 1998).

Moreover, the nucleus was strongly stained, probably as a result of over expression, with the exception of the nucleoli, K9R-A15R-stathmin presents strongly perinuclear staining which could be related with its highly expression level.

We examined the localization and phosphorylation level of site 16 in synchronized HeLa cells by a specific phosphorylation site-directed antiserum. Any staining is detectable in interphasic cells over expressed the two forms of stathmin, because it is low phosphorylated in interphase (Bieche et al., 2003).

Whereas the staining increases from prophase to metaphase and strongly decreases at cytokinesis in mitotic cells overexpressed WT-stathmin.

Serine 16 phosphorylation increases in prophase until metaphase and decreases in cytokinesis suggesting that CaMK-IV-Gr kinase protein is active on prophase and inactive on cytokinesis (Melander et al., 1997).

Mitotic cells overexpressed K9R-A15R-stathmin are low phosphorylated on site 16. These observations could be resulting from the second mutation (K15R) which creates a new hydrogen bound with site 16 in this stathmin form (data not shown). Stathmin is rapidly degraded after site 16 phosphorylation, the endogenous stathmin protein its half-life is more than 36 h, the mutant phosphorylated stathminCaMK-IV-Gr kinase protein is rapidly and continually induced during the 4h to 5h time course of the experiment (Melander et al., 1997).

We investigated the double mutation introduced and site 16 phosphorylation state dependences of the MT depolymerizing activity of stathmin *in vivo* by overexpressing WT-stathmin and K9R-A15R-stathmin.

In interphasic HeLa cells, it would appear lack of association of the two forms of stathmin with the MT network, which is in good agreement with its ability to interact with free tubulin rather than with polymerized MTs *in vitro* (Larsson et al., 1997).

Although, the alone N-terminal region of stathmin is able to depolymerize MT network in interphasic cells and opposites mitotic spindle formation (Segerman et al., 2003). The peptide I19L alone adopts a sophisticated β-hairpin structure in contact with tubulin in solution (Clement et al., 2005).

This could be resulting of perinuclear localization of K9R-A15R-stathmin enabling it to have an activity in interphasic cells; or rather that K9R-A15R-stathmin decreases the concentration of freetubulin.

In mitotic HeLa cells, it would appear lack of association of the WT-stathmin and MT network. During mitosis, stathmin is phosphorylation-inactivated by multisite phosphorylation by spindle assembly regulating kinase systems including CDK1, PLK1, and Aurora B (Gadea and Ruderman, 2006;Larsson et al., 1997). This indicates that stathmin activity is switched off until the spindle assembly checkpoint is silenced, which is consistent with the apparently normal spindle assembly in both human and murine somatic cells lacking stathmin (Holmfeldt et al., 2006;Ringhoff and Cassimeris, 2009). In contrast, K9R-A15R-stathmin reorganizes MTs into bundles at perinuclear area in cytokinesis cells. These observations could be linked to MT dynamic or stability and to its low phosphorylation state. MTs are reorganized

on bundles after taxol treatment (Gavet et al., 1998) which blocks the cell cycle in its G1 or M phases by stabilizing the MT cytoskeleton against depolymerization (Arnal and Wade, 1995). Otherwise, over expression of uphosphorylated stathmin mutant interfered with formation of the mitotic spindle in mitotic leukemia cells K562 by MTs bundles formation. Hence, phosphorylation of over expressed stathmin is essential to allow spindle formation during mitosis and subsequent cell division (Larsson et al., 1997).

Stathmin is overexpressed in various types of human cancers, including esophageal carcinoma, and its high expression levels could affect the distribution of cell cycle (Niethammer et al., 2004). Therefore, we studied the impact ofoverexpression of WT-stathmin and K9R-A15R-stathmin on synchronized HeLa cells proliferationusing MTT test.

Cell proliferation was measured by cell counting MTT at different times. At 19, 24 and 35h, the two forms of stathmin appear toxic compared to the control (transfected cells with p-EGFPN1 alone). These observations could be linked to the overexpression of stathmin in mitotic HeLa cells synchronized in G2/M phase where stathmin must be phosphorylated on its four phosphorylation site. Stathmin phosphorylation increases during the passage of G phase to S phase andevenduring the transition fromthe G2 phaseto mitosisin many cell types, such as K562 leukemic cells (Luo et al., 1994), Jurkat cells (Brattsand et al., 1994) or HeLacells (Bieche et al., 2003).

At 35 and 48 h, K9R-A15R-stathmin inhibits cell proliferation more than WT-stathmin which could be resulting for it higher expression and it low phosphorylation state in site 16 in mitotic cells.

Stathmin participates in the regulation of MT dynamic in relation with diverse biological regulations and in many cell types (Ozon et al., 1998).Analysis of dynamic at “plus” ends of MTs was studied by live fluorescence video microscopy in HeLa cells co-transfected with mcherry-EB3/Stathmin-GFP. The studied shows that the averages speed of “plus” ends moving are slowed in the presence of WT-stathmin and K9R-A15R-stathmin compared to the control. Stathmin appears change MTs “plus” end structure as has been shown interphasic Xenopus egg extracts by electron cryo-microscopy (Arnal et al., 2000). MT dynamic in mitotic cells is 10 times higher than in interphasic cells where it is less phosphorylated (Belmont et al., 1990). In other wise, in the presence of K9R-A15R-stathmin this sopped is slowed than the presence of WT-stathmin. It could be related with the double mutation introduced strengthen the bond between the N-terminal part of stathmin and tubulin, which increases the destabilizing activity of stathmin. High concentrations of the stathmin N-terminal portion increased the “catastrophe” rate during MT assembly *in vitro*. The N-terminal region of stathmin has autonomous activity. Evidently, this activity is enhanced by the increase in tubulin affinity that is provided by the extended a-helical portion of native stathmin (Segerman et al., 2003). Deletion of N-terminal region of stathmin resulted in a protein that retained tubulin-sequestering activity (Howell et al., 1999), but was unable to promote MT “catastrophes”.

CONCLUSIONS

In conclusion, we report here the involvement *in vivo* of the N-terminal region of stathmin in the stability of stathmin/tubulin interaction and the importance of stathmin activity regulation during cell proliferation byphosphorylation.We demonstrated thatthe double mutation (K9R-A15R) introduced at N-terminal region of stathmin had stabilized the interaction between stathmin and tubulin which strengthened its activity with MTs. Also, this double

mutation gave it new properties, including its expression or localization.

Furthermore, serine 16 phosphorylation during mitosis is critical for stathmin activity inhibition and its affinity reduction with tubulin. K9R-A15R-stathmin less phosphorylated on this site induces MT bundles formation and cell proliferation inhibition in mitotic HeLa cells.

Finally, we demonstrated N-terminal region function on MT dynamic regulation. K9R-A15R-stathmin reduces the elongation rate of MTs “plus” end by enhancing stathmin/tubulin binding. The role of stathmin is probably controlled by its specific molecular properties, as well as its expression, subcellular localization and phosphorylation profile.

ACKNOWLEDGEMENTS

S.Z. Tabet-Helal Bouali thanks the Algerian Government MESRS (Le Ministère de l'Enseignement Supérieur et de la Recherche Scientifique) for financial support during PhD period.

The author has not any financial or personal conflicts of interest.

REFERENCES

1. Anderson,D.J.,&Axel,R. (1985). Molecular probes for the development and plasticity of neural crest derivatives. Cell, 42, 649-662.
2. Arnal,I., Karsenti,E., & Hyman,A.A. (2000). Structural transitions at microtubule ends correlate with their dynamic properties in Xenopus egg extracts. J. Cell Biol, 149, 767-774.
3. Arnal,I.,&Wade, R.H. (1995). How does taxol stabilize microtubules? Curr. Biol, 5, 900-908.
4. Belmont,L.D., Hyman,A.A., Sawin,K.E., & Mitchison,T.J. (1990). Real-time visualization of cell cycle-dependent changes in microtubule dynamics in cytoplasmic extracts. Cell, 62, 579-589.
5. Belmont, L.D.,& Mitchison, T.J. (1996). Identification of a protein that interacts with tubulin dimers and increases the catastrophe rate of microtubules. Cell, 84, 623-631.
6. Beretta, L., Boutterin, M.C., & Sobel, A. (1988). Phosphorylation of intracellular proteins related to the multi hormonal regulation of prolactin: comparison of normal anterior pituitary cells in culture with the tumor-derived GH cell lines. Endocrinology, 122, 40-51.
7. Beretta, L., Dobransky, T., and Sobel, A. (1993). Multiple phosphorylation of stathmin. Identification of four sites phosphorylated in intact cells and in vitro by cyclic AMP-dependent protein kinase and p34cdc2. J. Biol. Chem, 268, 20076-20084.
8. Bieche, I.et al. (2003). Expression of stathmin family genes in human tissues: non-neural-restricted expression for SCLIP. Genomics, 81, 400-410.
9. Brattsand, G., Marklund, U., Nylander, K., Roos, G., & Gullberg, M. (1994). Cell-cycle-regulated phosphorylation of oncoprotein 18 on Ser16, Ser25 and Ser38. Eur. J. Biochem, 220, 359-368.
10. Charbaut, E., Curmi, P.A., Ozon,S., Lachkar,S., Redeker,V., & Sobel,A. (2001). Stathmin family proteins display specific molecular and tubulin binding properties. J. Biol. Chem, 276, 16146-16154.

11. Chneiweiss, H., Cordier, J., & Sobel,A. (1992). Stathmin phosphorylation is regulated in striatal neurons by vasoactive intestinal peptide and monoamines via multiple intracellular pathways. J. Neurochem, 58, 282-289.
12. Clement, M.J., Jourdain, I., Lachkar, S., Savarin, P., Gigant,B., Knossow, M., Toma,F., Sobel, A., &Curmi, P.A. (2005). N-terminal stathmin-like peptides bind tubulin and impede microtubule assembly. Biochemistry, 44, 14616-14625.
13. Curmi, P.A., Andersen, S.S., Lachkar, S., Gavet, O., Karsenti, E., Knossow, M., & Sobel, A. (1997). The stathmin/tubulin interaction in vitro. J. Biol. Chem, 272, 25029-25036.
14. Curmi, P.A., Gavet, O., Charbaut, E., Ozon, S., Lachkar-Colmerauer, S., Manceau, V., Siavoshian, S., Maucuer, A., &Sobel, A. (1999). Stathmin and its phosphoprotein family: general properties, biochemical and functional interaction with tubulin. Cell Struct. Funct, 24, 345-357.
15. David-Pfeuty, T., Erickson, H.P., & Pantaloni, D. (1977). Guanosinetriphosphatase activity of tubulin associated with microtubule assembly. Proc. Natl. Acad. Sci. U. S. A 74, 5372-5376.
16. Dorleans, A., Gigant, B., Ravelli, R.B., Mailliet, P., Mikol, V., & Knossow, M. (2009). Variations in the colchicine-binding domain provide insight into the structural switch of tubulin. Proc. Natl. Acad. Sci. U. S. A, 106, 13775-13779.
17. Doye, V., Boutterin, M.C., & Sobel, A. (1990). Phosphorylation of stathmin and other proteins related to nerve growth factor-induced regulation of PC12 cells. J. Biol. Chem, 265, 11650-11655.
18. Gadea, B.B., & Ruderman, J.V. (2006). Aurora B is required for mitotic chromatin-induced phosphorylation of Op18/Stathmin. Proc. Natl. Acad. Sci. U. S. A, 103, 4493-4498.
19. Gavet, O., Ozon, S., Manceau, V., Lawler, S., Curmi, P., & Sobel, A. (1998). The stathmin phosphoprotein family: intracellular localization and effects on the microtubule network. J. Cell Sci, 111 (Pt 22), 3333-3346.
20. Holmfeldt, P., Brannstrom, K., Stenmark, S., & Gullberg, M. (2006). Aneugenic activity of Op18/stathmin is potentiated by the somatic Q18-->e mutation in leukemic cells. Mol. Biol. Cell, 17, 2921-2930.
21. Howell, B., Larsson, N., Gullberg, M., & Cassimeris, L. (1999). Dissociation of the tubulin-sequestering and microtubule catastrophe-promoting activities of oncoprotein 18/stathmin. Mol. Biol. Cell, 10, 105-118.
22. Jourdain, L., Curmi, P., Sobel, A., Pantaloni, D., & Carlier, M.F. (1997). Stathmin: a tubulin-sequestering protein which forms a ternary T2S complex with two tubulin molecules. Biochemistry, 36, 10817-10821.
23. Koppel, J., Boutterin, M.C., Doye, V., Peyro-Saint-Paul, H., & Sobel, A. (1990). Developmental tissue expression and phylogenetic conservation of stathmin, a phosphoprotein associated with cell regulations. J. Biol. Chem, 265, 3703-3707.
24. Larsson, N., Marklund, U., Gradin, H.M., Brattsand, G., and Gullberg, M. (1997). Control of microtubule dynamics by oncoprotein 18: dissection of the regulatory role of multisite phosphorylation during mitosis. Mol. Cell Biol, 17, 5530-5539.

25. Larsson, N., Melander, H., Marklund, U., Osterman, O., & Gullberg, M. (1995). G2/M transition requires multisite phosphorylation of oncoprotein 18 by two distinct protein kinase systems. J. Biol. Chem, 270, 14175-14183.

26. le, G.S., Chneiweiss, H., Tarantino, N., Debre, P., & Sobel, A. (1991). Stathmin phosphorylation patterns discriminate between distinct transduction pathways of human T lymphocyte activation through CD2 triggering. FEBS Lett, 287, 80-84.

27. Liang, X.J., Choi, Y., Sackett, D.L., & Park, J.K. (2008). Nitrosoureas inhibit the stathmin-mediated migration and invasion of malignant glioma cells. Cancer Res, 68, 5267-5272.

28. Luo, X.N., Mookerjee, B., Ferrari, A., Mistry, S., & Atweh, G.F. (1994). Regulation of phosphoprotein p18 in leukemic cells. Cell cycle regulated phosphorylation by p34cdc2 kinase. J. Biol. Chem, 269, 10312-10318.

29. Manna, T., Thrower, D., Miller, H.P., Curmi, P., & Wilson, L. (2006). Stathmin strongly increases the minus end catastrophe frequency and induces rapid treadmilling of bovine brain microtubules at steady state in vitro. J. Biol. Chem, 281, 2071-2078.

30. Manna, T., Thrower, D.A., Honnappa, S., Steinmetz, M.O., & Wilson, L. (2009). Regulation of microtubule dynamic instability in vitro by differentially phosphorylated stathmin. J. Biol. Chem, 284, 15640-15649.

31. Marklund, U., Brattsand, G., Osterman, O., Ohlsson, P.I., &Gullberg, M. (1993). Multiple signal transduction pathways induce phosphorylation of serines 16, 25, and 38 of oncoprotein 18 in T lymphocytes. J. Biol. Chem, 268, 25671-25680.

32. Maucuer, A., Moreau, J., Mechali, M., & Sobel, A. (1993). Stathmin gene family: phylogenetic conservation and developmental regulation in Xenopus. J. Biol. Chem, 268, 16420-16429.

33. Melander, G.H., Marklund, U., Larsson, N., Chatila, T.A., & Gullberg, M. (1997). Regulation of microtubule dynamics by Ca2+/calmodulin-dependent kinase IV/Gr-dependent phosphorylation of oncoprotein 18. Mol. Cell Biol, 17, 3459-3467.

34. Mistry, S.J., & Atweh, G.F. (2002). Role of stathmin in the regulation of the mitotic spindle: potential applications in cancer therapy. Mt. Sinai J. Med, 69, 299-304.

35. Niethammer, P., Bastiaens, P., & Karsenti, E. (2004). Stathmin-tubulin interaction gradients in motile and mitotic cells. Science, 303, 1862-1866.

36. Ozon, S., Byk, T., & Sobel, A. (1998). SCLIP: a novel SCG10-like protein of the stathmin family expressed in the nervous system. J. Neurochem, 70, 2386-2396.

37. Ozon, S., Maucuer, A., & Sobel, A. (1997). The stathmin family -- molecular and biological characterization of novel mammalian proteins expressed in the nervous system. Eur. J. Biochem, 248, 794-806.

38. Ravelli, R.B., Gigant, B., Curmi, P.A., Jourdain, I., Lachkar, S., Sobel, A., &Knossow, M. (2004). Insight into tubulin regulation from a complex with colchicine and a stathmin-like domain. Nature, 428, 198-202.

39. Ringhoff, D.N., & Cassimeris, L. (2009). Stathmin regulates centrosomal nucleation of microtubules and tubulin dimer/polymer partitioning. Mol. Biol. Cell, 20, 3451-3458.

40. Rubin, C.I., & Atweh, G.F. (2004). The role of stathmin in the regulation of the cell cycle. J. Cell Biochem, 93, 242-250.

41. Schubart, U.K., Banerjee, M.D., & Eng, J. (1989). Homology between the cDNAs encoding phosphoprotein p19 and SCG10 reveals a novel mammalian gene family preferentially expressed in developing brain. DNA, 8, 389-398.

42. Segerman, B., Holmfeldt, P., Morabito, J., Cassimeris, L., & Gullberg, M. (2003). Autonomous and phosphorylation-responsive microtubule-regulating activities of the N-terminus of Op18/stathmin. J. Cell Sci, 116, 197-205.

43. Sobel, A. (1991). Stathmin: a relay phosphoprotein for multiple signal transduction? Trends Biochem. Sci, 16, 301-305.

44. Stein, R., Mori, N., Matthews, K., Lo, L.C., & Anderson, D.J. (1988). The NGF-inducible SCG10 mRNA encodes a novel membrane-bound protein present in growth cones and abundant in developing neurons. Neuron, 1, 463-476.

45. Steinmetz, M.O., Kammerer, R.A., Jahnke, W., Goldie, K.N., Lustig, A., &Van, O.J. (2000). Op18/stathmin caps a kinked protofilament-like tubulin tetramer. EMBO J, 19, 572-580.

46. Wang, S., Kurepa, J., Hashimoto, T., & Smalle, J.A. (2011). Salt stress-induced disassembly of Arabidopsis cortical microtubule arrays involves 26S proteasome-dependent degradation of SPIRAL1. Plant Cell, 23, 3412-3427.

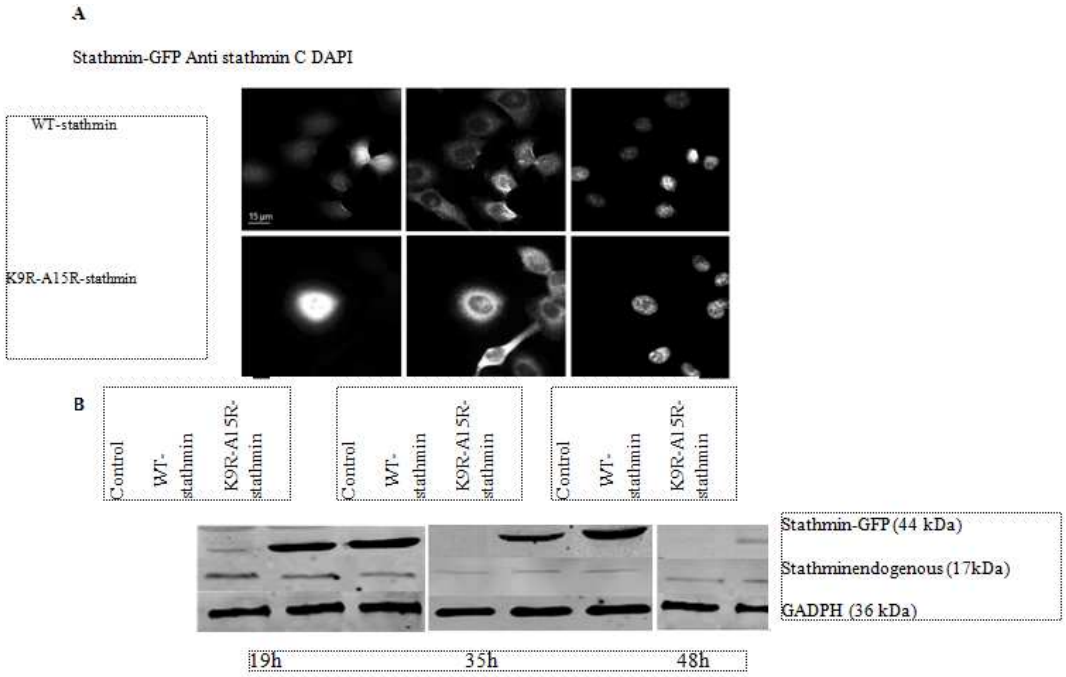

Figure 1: Immunolocalization and Immunoblotting of Stathmin in Synchronized HeLa Cells. (A) Cells were Transfected and Fixed with PFA 4% (See Materials and Methods) and Stained with Anti-Stathmin Antiserum C (1:500). DNA was Visualized by Co-Staining with DAPI. (B) Western Blotting Indicates the Expression Level of Stathmin Proteins. The Expression Level of Both Proteins is Distinct. GAPDH was used as a Loading Control

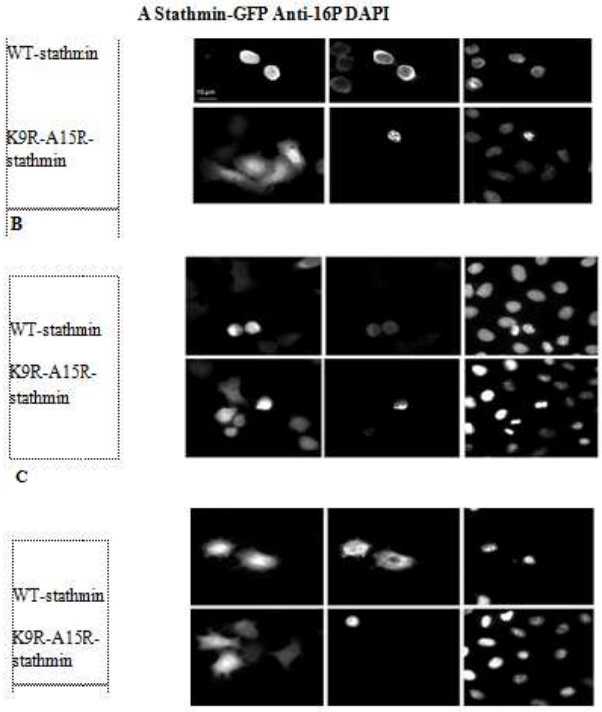

Figure 2: Immunostaining of Stathmin Anti-16P in Synchronized HeLa Cells. Cells were Transfected and Fixed with PFA 4% (See Materials and Methods) and Stained with Anti-Phosphorylated Serine 16 (1:10 000) at 19h (A), 35 h (B) and 48h (C). Only Mitotic Cells were Stained, DNA was Visualized by Co-staining with DAPI

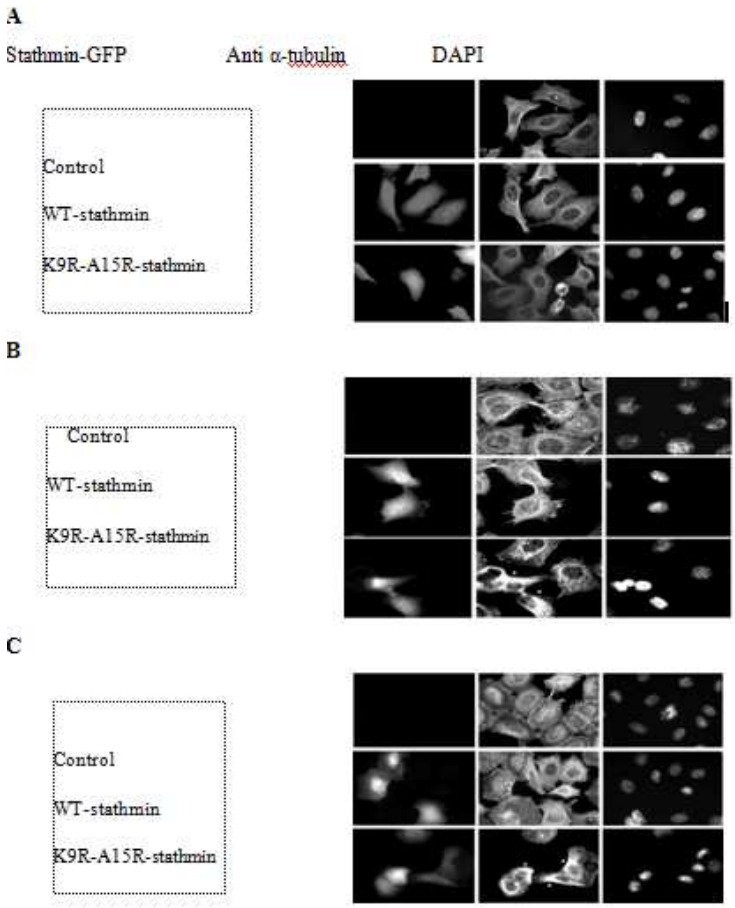

Figure 3: Effects of WT-Stathmin and K9R-A15R-Stathmin on the Interphasic and Mitotic MT Networks. Synchronized HeLa Cells were Transfected To Over Expressed WT Or K9R-A15R Stathmin and Fixed with PFA 4% (See Materials and Methods), and Stained with Anti A-Tubulin (1/3000) At 19 H (A), 35 H (B) Or 48 H (C). In Contrast to the WT-Stathmin, K9R-A15R-Stathmin Reorganizes MTs in Mitotic Cells on Bundles (Asterisks). DNA was Visualized by Co-Staining with DAPI

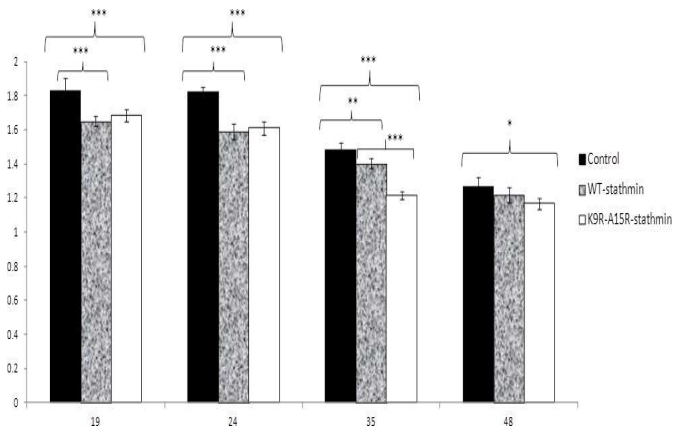

Figure 4: MTT Assay After WT-stathmin and K9r-a10r-stathmin Expression In Synchronized HeLa Cells. Data Are Shown Mean ± SLD from Three Independent Experiments, *p < 0.05, **p < 0.01 and ***p < 0.001

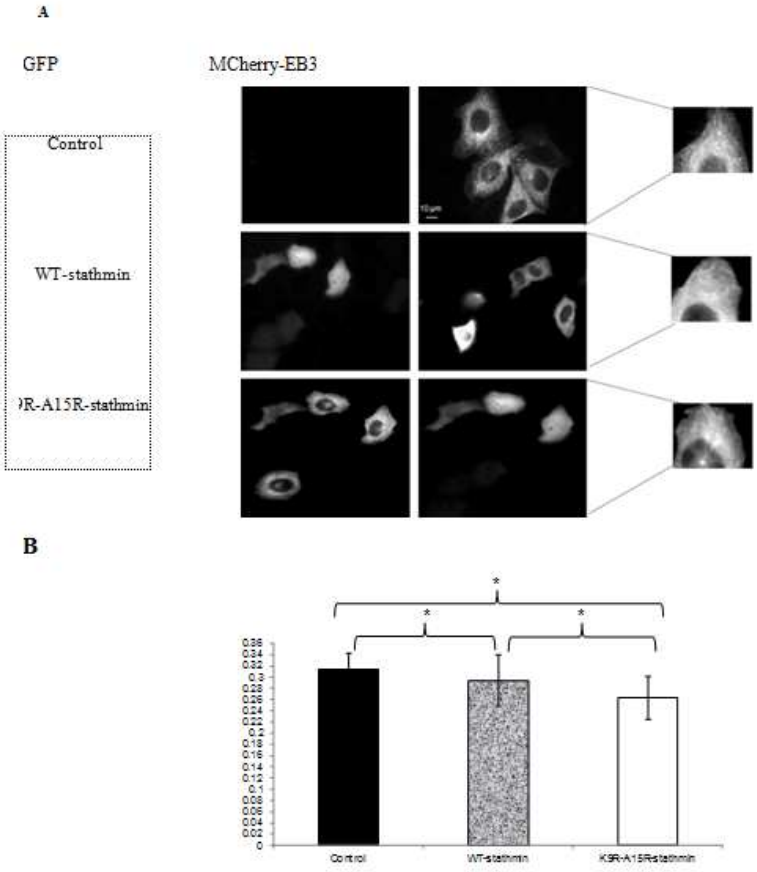

Figure 5: MCherry-EB3 Localization and Observation in HeLa cells. (A) EB3 Comets were Observed by Live Fluorescence Video Microscopy. Representative Cells Correspond to Green Fluorescence (stathmin-GFP) and to Red Fluorescence (RFP-EB3). (B) Movements of MTs « Plus » End in Transfected HeLa cells. Data are Shown Mean ± SLD from Three Independent Experiments. *P < 0.05